TITLE

Photodynamic Therapy Compounds

FIELD OF INVENTION

The invention relates to compounds for photodynamic therapy (PDT) of cancerous and other diseased tissue.

Among known PDT compounds are those of USP 4,837,221 and USP 4,992,257 the disclosure of which is incorporated herein by reference.

The disclosure of '221' includes porphyrins of the formula:

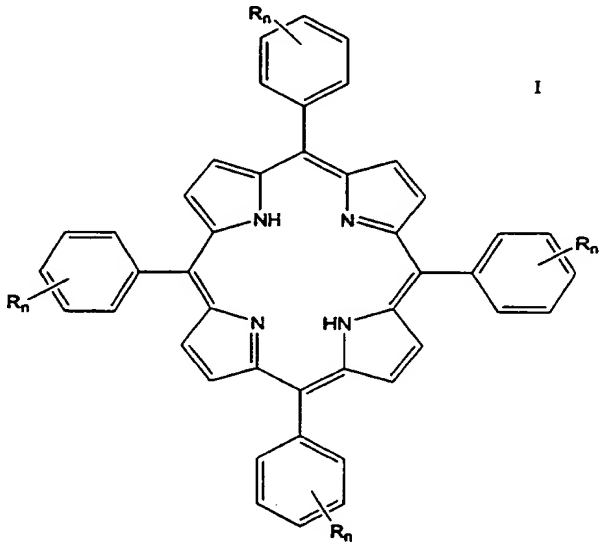

I

where n=1 to 3 and each substituent R in the phenyl rings, or other aryl groups replacing phenyl, is a hydroxy group. Particularly noted are those compounds where each substituent is o-hydroxyphenyl, m-hydroxyphenyl or p-hydroxyphenyl.

The disclosure of '257' includes di-hydro porphyrins (chlorins), and corresponding tetra-hydro porphyrins (bacteriochlorins) of the formulae:

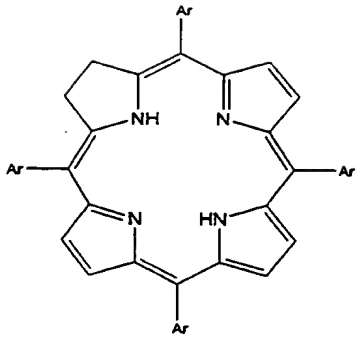

II

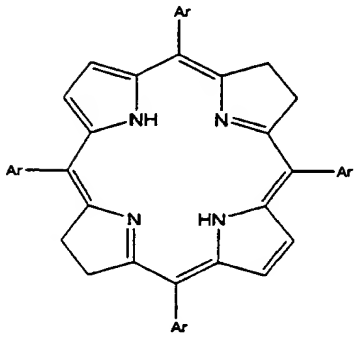

III

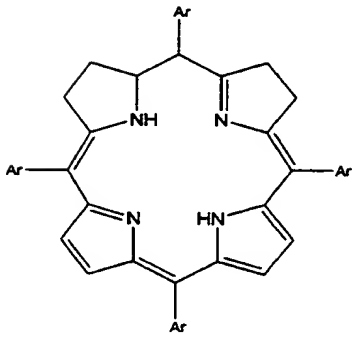

IV

wherein each Ar is an aromatic group with one or more hydroxy substituent groups but as with '221' is desirably phenyl. Preferred compounds are m-THPC, meta tetra(hydroxyphenyl) chlorin, currently in FDA trials, and the corresponding bacteriochlorin.

As will be recognized, the above formulae show in each case one only of the possible imino-nitrogen tautomers; possible tautomers include for chlorins:-

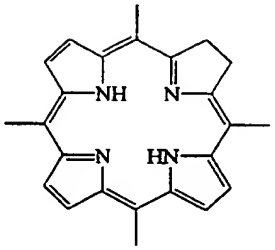

VA

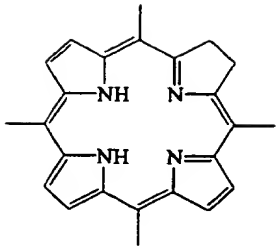

VB

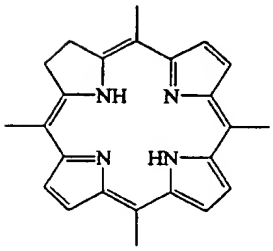

VC

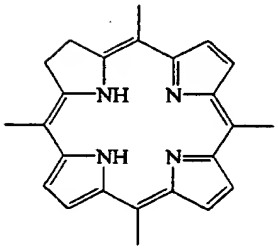

VD

for bacteriochlorins:-

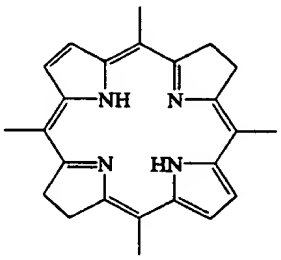

VIA

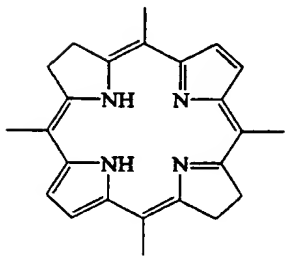

VIB

and for isobacteriochlorins:-

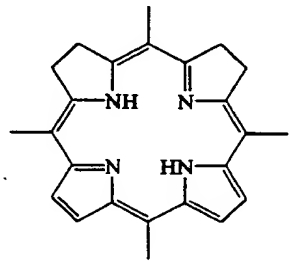

VIIA

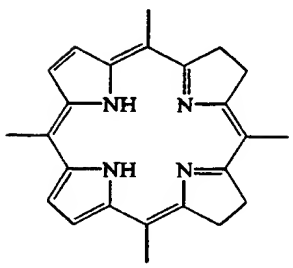

VIIB

THE INVENTION

We have sought improvements to PDT compounds and propose linking (conjugating) them to antibodies including active antibody fragments, specific to antigens of a diseased tissue. In particular, a number of monoclonal antibodies (Mabs) are available targeted to cancerous cells and we have found that they can be chemically linked to PDT compounds to give valuable PDT therapies.

More particularly the invention provides compounds where a ring structure

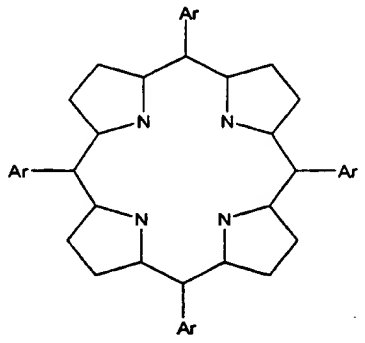

VIII

representing a porphyrin, chlorin or bacteriochlorin/isobacteriochlorin ring in any of its imino-nitrogen tautomeric forms, carries four aromatic preferably phenyl substituents Ar each themselves carrying one or more hydroxy groups, one or more of which hydroxy groups is in turn linked to an antibody (in which are included antibody fragments) reactive to a cancer or other diseased -cell antigen, giving a conjugate valuable in PDT therapy of the disease. The preferred aromatic substituent is m-hydroxy phenyl, as in m-THPC.

In principle the antibodies can be linked direct to the hydroxy groups but generally the presence of a linking group is preferred. Examples are ether-linked groups for example

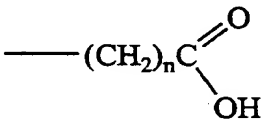

or —$(CH_2)_n$-A

where n is 1 to 4 and A is –OH or $–NH_2$

or, less preferred, ester-linked groups for example:-

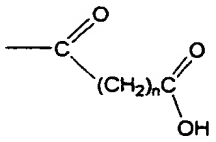

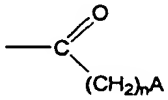

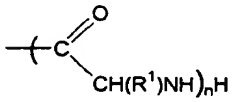

where n and A are as before and R^1 is hydrogen or a hydrocarbon or carboxylated amino-acid side chain, representing particularly glycine, alanine, lysine or glutamic acid.

Ester, amide or other links are then readily formed with the antibody according to the free reactive groups present on it.

The invention extends to compounds as in VIII but carrying such linking groups, as intermediates, as well as to the antibody conjugates themselves.

The invention further relates to the treatment of disease by PDT using the antibody conjugates and to the use of antibody conjugates in the preparation of medicaments for PDT.

It is believed, though the invention is not restricted to any mechanism, that in use of the conjugates they or at least the PDT active are internalized by the cells of diseased tissue after administration of the conjugate.

The mechanism of action of PDT agents is believed to be that they destroy mitochondrial function by the generation of free radicals and/or reactive oxygen species. Such free radicals or reactive oxygen species need to reach the mitochondria, which are within the cytoplasm, and it is supposed that for photodynamic therapy to be active, the PDT molecule has to penetrate the cell

surface membrane and be energized in close proximity to the mitochondria. The free radicals and reactive oxygen species then do the damage.

However, it may equally be that if adequate PDT conjugate binds to cell membranes and is energized there, then the free radicals and reactive oxygen species can penetrate the cell surface membrane thereafter destroy the mitochondria.

The antibodies will normally be monoclonal antibodies of which mMAB 425 discussed in detail herein is an example. There are many such antibodies known, directed against cell surface antigens of cancer or other disease cells. Examples include

Antigen	Target
CD19	Lymphoma
CD20	Lymphoma/chronic lymphocytic leukemia/non-Hodgkin lymphoma (NHL)
CD22	NHL
CD33	Acute pro myelocytic leukemia
CD45	Leukemia
CD40	Leukemia
	Target (solid tumors)
HLADR (lyml)	Lymphoma/CLL
Lewis Y	Breast
Integrin receptor	Breast
PEM (MUCI)	Breast
HER2/erB2/neu	Breast
CEA	Epithelial (colon)
VEGF	Epithelial
α cell surface glycoprotein	Epithelial (colon)
EGF-r	Breast, renal, pancreatic, H&N, lung
TNT	Lung, pancreas, gastric, colon, breast

PSMA	Prostate
TAG-72	Ovarian
CD56	Small-cell lung carcinoma
PLAP	Ovarian, cervical, testis

The chemistry of the conjugation of the actives and antibodies depends on their nature and on whether a linking group is used and is not central to the invention in its broad sense. However, chemistry as described herein for m-THPC is suitable for other chlorins and also for porphyrins and bacteriochlorins/isobacteriochlorins, particularly the m-hydroxy phenyl derivatives corresponding to m-THPC.

Particular aspects of the invention are described in detail below, giving first a summary and general discussion, largely with reference to m-THPC conjugates, and then going on to materials and methods, to results, and to further discussion, all again largely in relation to m-THPC.

SUMMARY

A limitation of photodynamic therapy (PDT) is the lack of tumor selectivity of the photosensitizer. To overcome this problem, a protocol has been developed for coupling of *meta*-tetrahydroxyphenylchlorin (*m*THPC), one of the most promising photosensitizers, to tumor selective monoclonal antibodies (MAbs). *m*THPC was radiolabeled with ^{131}I to facilitate the assessment of the *in vitro* and *in vivo* behavior. After modification to ^{131}I-*m*THPC-(CH_2CO-$OH)_4$, thus increasing the water solubility and creating a functional moiety suitable for coupling, conjugation was performed using a labile ester. Insoluble aggregates were not formed when *m*THPC-MAb conjugates with a molar ratio of up to 4 were prepared. These conjugates showed a minimal impairment of the integrity on SDS-PAGE, full stability in serum *in vitro* and an optimal immunoreactivity.

For testing of the *in vivo* behavior of the *m*THPC-MAb conjugates the head and neck squamous cell carcinoma (HNSCC) selective chimeric MAb (cMAb) U36 was used in HNSCC bearing nude mice. Biodistribution data showed that the tumor selectivity of cMAb U36-conjugated *m*THPC was increased in comparison with free *m*THPC, despite the fact that conjugates with a higher *m*THPC:MAb ratio were more rapidly cleared from the blood.

Preliminary results on the *in vitro* efficacy of PDT with MAb-conjugated *m*THPC showed that *m*THPC coupled to the internalizing murine MAb (mMAb) 425 exhibited more phototoxicity than when coupled to the non-internalizing cMAb U36

GENERAL DISCUSSION

Photodynamic therapy (PDT) is a therapeutic modality for the treatment of superficially localized tumors. In this approach a photosensitive dye (photosensitizer) is injected intravenously, whereafter it accumulates more or less selectively in the tumor. After exposure to laser light in the red or near-infrared region, the sensitizer is excited and is able to produce singlet oxygen, a cytotoxic form of oxygen. Direct cell killing, occlusion of tumor blood vessels as well as a strong acute inflammatory reaction can occur. These combined effects result in tumor necrosis. PDT has been applied for non-invasive treatment of many types of cancer, including colon, bladder, lung, and head and neck cancer.

Various photosensitizers have recently become available. One of the most promising second generation photosensitizers is *meta*-tetrahydroxyphenylchlorin (*m*THPC). *m*THPC is a pure and well-defined compound. It has a strong absorption band at 652 nm (absorption coefficient 22400 $l.mol^{-1}.cm^{-1}$, compared with 3000 for Photofrin at 630 nm). The longer wavelength light used to excite *m*THPC can penetrate deeper into the tissue than 630 nm light, thus allowing treatment of larger tumors. The high photochemical efficiency of *m*THPC means that lower light doses (and shorter illumination times) are required for a tumoricidal PDT effect.

Preliminary results of PDT with *m*THPC in head and neck cancer patients are encouraging (1). The largest study has been performed by Savary *et al.* using optimized protocols for PDT with *m*THPC for the treatment of early second primary squamous cell carcinoma of the esophagus, bronchi and mouth (2). All lesions were carcinoma *in situ* or microinvasive carcinoma which had been detected by rigid endoscopy and toluidine blue as a vital stain. Of the 33 lesions treated in this trial, 28 showed no recurrence during the mean follow-up of 14 months. In comparison to surgery and radiotherapy, PDT shows a low morbidity with little fibrosis and scarring.

Despite these promising results, *m*THPC-based PDT leaves room for improvement. A limitation is the lack of tumor selectivity, which can result in severe normal tissue damage after PDT of large surface areas. An option to overcome this problem is to couple *m*THPC to monoclonal antibodies (MAbs) directed against tumor-associated antigens. In this way the photosensitizer will be targeted selectively to the tumor. These *m*THPC-MAb conjugates are especially suitable for the treatment of multiple tumor foci in large areas, as is the case in minimal residual disease after surgical resection of thoracic and peritoneal tumors. The problem of phototoxicity is also reduced since the accessibility of the skin is limited for MAbs.

In the development of photoimmunoconjugates for therapy the synthesis of *m*THPC-MAb conjugates has not yet been described. A serious problem in this respect is the poor water solubility of *m*THPC. Other factors expected to hamper the development of *m*THPC-MAb conjugates suitable for tumor targeting are the potential chemical crosslinking during conjugation, as well as the impairment of the immunoreactivity and pharmacokinetic behavior of the MAb and the photochemical activity of the conjugates.

We have focused on the use of MAbs for selective targeting of squamous cell carcinoma of the head and neck (HNSCC). To this end MAbs E48 and U36 have been developed (3,4). Radioimmunoscintigraphy/biodistribution studies in HNSCC patients showed that these MAbs are highly capable of selective tumor targeting (5,6,7). This observation justifies a study for the use of these MAbs as transport vehicle for selective delivery of *m*THPC to HNSCC.

In this application we describe a protocol for the reproducible synthesis of *m*THPC-MAb conjugates and their biodistribution after administration to HNSCC-bearing nude mice. Conjugation and biodistribution studies were performed with dual labeling using ^{131}I-labeled *m*THPC and ^{125}I-labeled MAb. Preliminary data on the *in vitro* efficacy of *m*THPC-MAb mediated PDT are provided.

MATERIALS AND METHODS

***m*THPC.** *Meta*-tetrahydroxyphenylchlorin (*m*THPC; M_r=680.76) was obtained from Scotia Pharmaceuticals (Stirling, UK) as a pure solid. [^{14}C]*m*THPC (also provided by Scotia Pharmaceuticals) was synthesized by American Radiolabeled Chemicals Inc. (St. Louis, USA).

Monoclonal Antibodies. Selection and production of MAb U36 and its chimeric (mouse/human) IgG1 derivative (cMAb U36) have been described previously (4, 8). MAb U36 recognizes the v6 domain of the 200 kDa CD44 splice variant epican (9), which is highly expressed in squamous cell carcinoma of the head and neck, lung, skin, oesophagus and cervix, adenomacarcinomas of breast and lung, as well as in normal stratified epithelium. A clinical RIS study with ^{99m}Tc-labeled U36 revealed that U36 IgG accumulates selectively and to a high level in HNSCC (7), and therefore the MAb is currently evaluated in RIT studies.

Murine monoclonal antibody 425 (mMAb 425) is a IgG2a MAb developed and characterized by Murthy *et al.* (10). The epitope recognized by mMAb 425 is localized on the external domain of the EGF receptor (EGFR), which has been shown to be highly expressed by various tumor types including HNSCC, renal cell cancer, gliomas and carcinoma of the oesophagus, bladder, cervix, stomach, lung and breast. After binding to this antigen, anti-EGFR MAbs are internalized and catabolized by A431 cells (11). Anti-EGFR MAbs, MAb 425 included, have been extensively studied in clinical trials (12,13).

Cell Lines. Characteristics of the squamous cell carcinoma cell lines UM-SCC-11B, UM-SCC-22A and A431 and their culturing conditions are known in the art.

Analyses. HPLC analysis was performed by using a LKB 2150 HPLC-pump (Pharmacia Biotech, Roosendaal, The Netherlands), a LKB 2152 LC controller (Pharmacia Biotech) and a 25-cm Lichrosorb 10 RP 18 column (Chrompack, Middelburg, The Netherlands) at a flow-rate of 2 ml/min. The eluant consisted of a 9:1 (v/v) mixture of MeCN and 0.1% trifluoroacetic acid. Absorption was measured at 230 nm and 415 nm by a Pharmacia LKB VWM 2141 UV detector. Radioactivity was measured by an Ortec 406A single-channel analyzer connected to a Drew 3040 Data collector (Betron Scientific, Rotterdam, The Netherlands).

Proton nuclear magnetic resonance (^{1}H-NMR) spectra were recorded in [^{2}H$_6$]Me$_2$SO on a Bruker ARX 400 (400.14 MHz) spectrometer and a Bruker AC 200 (200.13 MHz)

spectrometer. Chemical shifts (δ) are given in ppm relative to tetramethylsilane as the internal standard. For description of the NMR spectra of *m*THPC and its derivatives see Table 1.

TABLE 1. Chemical Shifts (ppm) of *m*THPC, *m*THPC-(CH_2COOH)$_4$ and *m*THPC-(CH_2CO-TFP)$_4$

	O*H* (s)	pyrrole-C*H*	TFP-*H* (m)	benz.--*H* (m)	-C*H*$_2$CO- (d)	pyrrole-C*H*$_2$ (s)	NH (s)
number of protons	4	6	4	16	8	4	2
*m*THPC	9.81	8.68[1]/8.42/ 8.28[2] (d/s/d)		7.65-7.12		4.20	-1.60
*m*THPC-(CH_2COOH)$_4$	11.30	8.62[3]/8.37/ 8.24[4] (d/s/d)		7.66-7.20	4.83[8]	4.17	-1.64
*m*THPC-(CH_2CO-TFP)$_4$		8.60[5]/8.35[6]/8.21[7] (dd/d/dd)	7.96	7.79-7.39	5.57[9]	4.13	-1.60

Note: s = singlet; d = doublet; dd = double doublet; m = multiplet.
Observed coupling constants (Hz): 1: J=4.9; 2: J=4.9; 3: J=5.4; 4: J=5.4; 5: J=5.2; 6: J=4.3; 7: J=5.1; 8: J=10.1; 9: J=12.7.

The absorption spectra of *m*THPC and *m*THPC-MAb conjugates were measured using a Ultrospec III spectrophotometer (Pharmacia Biochrom). The *m*THPC concentration in the conjugate preparations was assessed with the same apparatus at a wavelength of 415 nm. The absorption of a range of dilutions (1-9 μg/ml) of *m*THPC in MeCN was measured and

graphically depicted using the least square method. The *m*THPC concentration in the conjugate preparations was determined using this calibration curve.

The integrity of the *m*THPC-MAb conjugates was analyzed by electrophoresis on a Phastgel System (Pharmacia Biotech) using preformed 7.5% SDS-PAGE gels under non-reducing conditions. After running, gels were stained with 0.2% Coomassie Brilliant Blue (CBB, Sigma) and exposed to a Phosphor plate for 1-3 h and analyzed with a Phosphor Imager (B&L-Isogen Service Laboratory, Amsterdam) for localization of the protein bands. Quantitative information was obtained by cutting the lanes into pieces and dual label counting in a gamma counter (LKB-Wallac 1282 CompuGamma, Pharmacia, Woerden, The Netherlands).

Dual Label Counting of ^{125}I and ^{131}I. The amounts of ^{125}I (E_γ 35 keV) and ^{131}I (E_γ 364 keV) were measured simultaneously in a gamma counter in the corresponding window settings (channels 35-102 and 155-185, respectively) with automatic correction for the ^{131}I-comptongammas in the ^{125}I-window setting; in our case this correction corresponded to 15.2% of the ^{131}I-photopeak counts present in the sample.

^{125}I-Labeling of MAbs. Radioiodination of cMAb U36 and mMAb 425 with ^{125}I was performed using Iodogen (Brunschwig Chemie, Amsterdam) as described by Haisma *et al.* . 1-2 mg MAb dissolved in 500 µl PBS (pH 7.4) and 1 mCi ^{125}I (100 mCi/ml, Amersham, Aylesbury, England) were mixed in a vial coated with 50 µg Iodogen. After 5 min incubation at room temperature the reaction mixture was filtered through a 0.22 µM Acrodisc filter (Gelman Sciences Inc., Ann Arbor, MI) and unbound ^{125}I was removed using a PD-10 column (Pharmacia Biotech, Woerden) with 0.9% NaCl as eluant. After removal of unbound ^{125}I, the radiochemical purity always exceeded 98%.

^{131}I-Labeling of *m*THPC. To facilitate the analysis of the stability of the *m*THPC-MAb conjugates *in vitro* and *in vivo*, and their pharmacokinetic behavior, in most of the experiments *m*THPC was trace-labeled with ^{131}I. This labeling and subsequent reaction steps with *m*THPC were carried out in the dark and under a N_2 atmosphere to prevent unwanted photochemical reactions during the synthesis of the *m*THPC-MAb conjugates.

^{131}I-Labeling of *m*THPC was performed using Iodo-beads (Brunschwig Chemie) as follows: the appropriate amount of ^{131}I was added to 50 µl of 1 mM NaOH containing 10 µg Na_2SO_3. This ^{131}I-solution was added to 4 Iodo-beads covered with 450 µl of a MeCN/H_2O mixture (10:1; v/v) followed by 100 µl (734 nmol) of a *m*THPC-solution (5 mg/ml in MeCN). After labeling during 30 min the reaction mixture was diluted with 400 µl H_2O, loaded on a conditioned Sep-pak C_{18} cartridge (Waters, Millipore, MA) and washed with 50 ml H_2O. The ^{131}I-labeled *m*THPC (actually consisting of a small proportion of ^{131}I-*m*THPC and an excess of unlabeled *m*THPC) was eluted with 3 ml MeCN. The solvent was evaporated under a stream of N_2.

The radiochemical purity of ^{131}I-*m*THPC was determined by HPLC analysis. The HPLC retention times were: 9.8 min for ^{131}I-*m*THPC, between 5-9 min for ^{131}I-labeled minor impurities and 9.6 min for *m*THPC (For the ^{1}H-NMR data of *m*THPC see Table 1).

Preparation of the Tetrafluorophenol (TFP) Ester. Preparation of the ester (either in labeled or unlabeled form) was performed in two steps. The first step was tetra-carboxymethylation of ^{131}I-*m*THPC/*m*THPC. To ^{131}I-*m*THPC/*m*THPC, dissolved in 600 µl of a DMF/H_2O mixture (5:1; v/v), 150 mg (3.7 mmol) powdered NaOH were added and the mixture was stirred until the solution was green (2-3 min). Hereafter, 70 mg (380 µmol) of iodoacetic acid (Janssen Chimica, Beerse, Belgium) were added and stirring was continued for another 90 min. The pH was adjusted to 5.0 with 3 ml of 1 N HCl, and the tetracarboxymethylated product was isolated by extraction with four portions of 0.5 ml CH_2Cl_2. The HPLC retention times were: 7.1 min for ^{131}I-*m*THPC-$(CH_2COOH)_4$ and 7.3 min for *m*THPC-$(CH_2COOH)_4$ (^{1}H-NMR data of *m*THPC-$(CH_2COOH)_4$ are given in Table 1).

In the next reaction step the four carboxylic acid groups were esterified using an excess of TFP (Janssen Chimica). To the tetracarboxymethylated product in CH_2Cl_2 150 µl of a TFP-solution (100 mg/ml in DMF) and 50 mg solid EDC (Janssen Chimica) were added. The pH was adjusted to 5.7-5.9 with 1 N Na_2CO_3. After reaction for 30 min, column chromatography was performed to remove all impurities. This purification was performed with a 24 cm LiChroprep Si 60 (40-63 µm) column (Merck, Darmstadt, Germany) using CH_2Cl_2/MeCN

(97:3; v/v) as the eluant (flow rate of 1 ml/min). Fractions of 0.5 ml were collected and analyzed by HPLC with absorption measurement at 230 and 415 nm. The pure tetra-ester fractions (under our conditions fractions 20-23) were pooled and the solvent was evaporated. The HPLC retention times were: 17.2 min for ^{131}I-*m*THPC-(CH_2CO-TFP)$_4$ (Fig. 2B) and 15.9 min for *m*THPC-(CH_2CO-TFP)$_4$ (Fig. 2A; ^{1}H-NMR data of *m*THPC-(CH_2CO-TFP)$_4$ are given in Table 1).

Preparation of ^{131}I-*m*THPC-(CH_2COOH)$_3CH_2CONH$-^{125}I-MAb Conjugates. For the coupling reaction with the ^{125}I-labeled MAb the ^{131}I-*m*THPC-(CH_2CO-TFP)$_4$ (Fig. 2A and B) was partly hydrolyzed in order to leave one reactive ester function thus preventing crosslinking of MAbs during conjugation. The partial hydrolysis was performed by dissolving the tetra-ester in 300 µl MeCN and by stepwise addition of 10-25 µl 10 mM Na_2CO_3. The degree of hydrolysis was monitored by radio-HPLC analysis with simultaneous absorption measurement at 415 nm (Fig. 2C and D). When the percentage of mono-ester was optimal for conjugation (no tetra- and tri-ester, less than 5% di-ester, 45% mono-ester together with 50% completely hydrolyzed ^{131}I-*m*THPC-(CH_2COOH)$_4$, Fig. 2E and F), this mixture was added to 2 mg ^{125}I-labeled MAb in 1 ml 0.9% NaCl at pH 9.5. After 30 min incubation, the ^{131}I-*m*THPC-(CH_2COOH)$_3CH_2CONH$-^{125}I-MAb conjugate was purified by gel filtration using a PD-10 column with 0.9% NaCl as eluant.

The conjugation efficiency was determined from the ^{125}I:^{131}I ratio before and after PD-10 purification using dual label counting in a gamma counter. The ^{131}I-*m*THPC:^{125}I-MAb molar ratio was determined by measuring the absorbance at 415 nm to calculate *m*THPC concentration and ^{125}I measurement for MAb quantitation. The integrity of the conjugate was checked by gel electrophoresis.

The chemistry is summarised in Figure 1. Repeating the chemistry but starting with the porphyrins of USP 4,837,221, particularly o-, p- or m-THPP corresponding to o-, p- or m-THPC, or with the bacteriochlorins or isobacteriochlorins of USP 4,992,257, particularly o-, p- or m-THPB or THPiB corresponding to o-, p- or m-THPC, gives the mMAB 425 conjugates of those compounds.

***In Vitro* Stability and Immunoreactivity of ^{131}I-*m*THPC-^{125}I-MAb Conjugates[2]**. For measurement of the serum stability of the ^{131}I-*m*THPC-^{125}I-MAb conjugates, 0.5 µg conjugate

in 10 µl 0.9% NaCl was added to 40 µl serum. Stability was measured in mouse and human serum, while 0.9% NaCl served as a control. After 20 h incubation in the dark at 37°C, samples were analyzed with SDS-PAGE. Quantitative information was obtained by cutting the lanes into pieces and dual label counting.

In vitro binding characteristics of ^{131}I-*m*THPC-^{125}I-MAb conjugates were determined in an immunoreactivity assay as described by Lindmo *et al.* and compared with those of the unconjugated ^{125}I-MAb. UM-SCC-11B cells were used for ^{125}I-cMAb U36 and A431 cells for ^{125}I-mMAb 425.

Biodistribution Studies. The biodistribution of ^{125}I-cMAb U36 and ^{131}I-*m*THPC-^{125}I-cMAb U36 conjugate was studied in nude mice bearing s.c. xenografts of the HNSCC cell line HNX-OE, tumor size ranging from 50 to 200 mm^3. For a comparison the distribution of ^{131}I-*m*THPC-$(CH_2COOH)_4$, ^{123}I-*m*THPC and [^{14}C]*m*THPC (as a reference compound used by others) was studied in the same animal model. Because the latter two compounds were coinjected in the same group of animals, the short-living ^{123}I-isotope was used instead of ^{131}I to facilitate the assessment of the ^{14}C activity.

The cMAb U36 samples were injected i.v. in 0.9% NaCl; the ^{123}I- and [^{14}C]*m*THPC derivatives in a mixture consisting of 20% EtOH, 30% polyethylene glycol 400 and 50% water (v/v). At indicated time points post-injection, mice were anesthetized, bled, killed and dissected. The urine was collected and the organs were removed. After weighing, the amount of gamma-emitting radioactivity in organs, blood and urine was measured in a gamma counter.

For the weak β-emitter ^{14}C, the blood, urine and organs were treated as follows: after complete decay of ^{123}I, tissue samples were placed in counting vials and 1 ml of Soluene-350 (Packard Instrument Company, Groningen, The Netherlands) was added to dissolve the organs. The vials were subsequently heated at 50°C for 24 h, after which 250 µl of a 1:1 (v/v) mixture of 30% H_2O_2 and acetic acid was added for decolorization of the solutions. After 1 h Ultima Gold liquid scintillation cocktail (15 ml, Packard Instrument Company) was added to the samples prior to counting in a LKB-Wallac 1410 Liquid Scintillation Counter (Pharmacia,

Woerden). Radioactivity uptake in the tissues was expressed as the percentage of the injected dose per gram of tissue (%ID/g).

Photoimmunotherapy *in vitro*. Phototoxicity of the *m*THPC-cMAb U36 conjugates and the unconjugated *m*THPC was assessed in UM-SCC-22A cells using the sulforhodamine B (SRB, Sigma) assay, which measures the cellular protein content. Cells were plated in 96-well plates (2500 per well) and grown for 3 days before incubating with *m*THPC or *m*THPC-cMAb U36 conjugates (0.1 nM to 1.0 μM *m*THPC equivalent) in DMEM supplemented with 2 mM L-glutamine, 5% FCS and 25 mM HEPES at 37 °C. After 20 h remaining free *m*THPC-cMAb U36 and *m*THPC were removed by washing twice with medium. Fresh medium was added and cells were illuminated at 652 nm with a 6 W Diode Laser (AOC Medical Systems) at a dose of 25 J/cm^2. Three days after illumination, growth was assessed by staining the cellular proteins with SRB and spectrophotometric measurement of the absorption at 540 nm with a microplate reader. IC_{50} values were estimated based on the absorption values and defined as the concentration that corresponded to a reduction in growth of 50% compared with values for control cells (no *m*THPC-MAb conjugates or *m*THPC added but illuminated in the same way).

Phototoxicity of the *m*THPC-mMAb 425 conjugates was assessed in A431 cells (2000 cells/well) in a similar way.

RESULTS

Iodination of *m*THPC. The first step in the synthesis of ^{131}I-*m*THPC-$(CH_2COOH)_3CH_2CONH$-^{125}I-MAb conjugates (**5**, Fig. 1) was trace-labeling of *m*THPC with ^{131}I using Iodo-beads. After 30 min incubation at room temperature, HPLC analysis revealed 70-75% ^{131}I-*m*THPC (**1**, Fig. 1), less than 10% ^{131}I-labeled impurities and about 20% unreacted ^{131}I. After purification on a Sep-pak cartridge the final preparation contained >94% ^{131}I-*m*THPC, less than 4% impurities and about 2% unbound ^{131}I.

Synthesis of ^{131}I-*m*THPC-$(CH_2CO$-TFP$)_4$. In the next step, ^{131}I-*m*THPC was tetra-carboxymethylated. The reaction with an excess of iodoacetic acid at pH 13, followed by extraction with CH_2Cl_2, gave 95% ± 5% (HPLC analysis) tetracarboxymethylated product (**2**,

Fig. 1). Esterification was performed with TFP and purification of the crude product with a LiChroprep column gave the desired product (3, Fig. 1) with >95% purity, also containing <5% ^{131}I-*m*THPC-(CH_2CO-TFP)$_3$.

The purity of the fractions (0.5 ml) that were recovered from the LiChroprep column was analyzed using HPLC analysis at 415 nm for detection of *m*THPC-(CH_2CO-TFP)$_4$ and at 230 nm for detection of ICH_2CO-TFP, formed as a side-product. On the LiChroprep column this latter ester had a retention time slightly longer than *m*THPC-(CH_2CO-TFP)$_4$. The fractions that only contained *m*THPC-(CH_2CO-TFP)$_4$ (under our conditions fractions 20-23) were, after collection, evaporated under a stream of N_2 and stored in the dark at 4 °C until use. The LiChroprep purification also removed unbound ^{131}I, and any unreacted TFP, EDC or ICH_2COOH. As a result, the *m*THPC-ester was obtained in an overall yield of 60% with a purity >95%.

Conjugation. The ^{131}I-*m*THPC-(CH_2CO-TFP)$_4$ ester was dissolved in 300 µl MeCN before starting of the HPLC-monitored hydrolysis with 10 mM Na_2CO_3-buffer. This base was added in portions of 10-25 µl with intervals of 10 min. Approximately 125-150 µl of this buffer was used to reach the optimum mixture for conjugation (4, Fig. 1).

For conjugation the mixture was added to a solution of ^{125}I-MAb in 0.9% NaCl at pH 9.5. After 30 min at room temperature the ^{131}I-*m*THPC-(CH_2COOH)$_3CH_2CONH$-^{125}I-MAb conjugate (5, Fig. 1) was purified on a PD 10 column. When 2 mg ^{125}I-MAb in a conjugation volume of 1.8 ml was used, the ^{131}I-*m*THPC-^{125}I-MAb molar ratio was about 2.0-2.5. The conjugation efficiency was 60% ± 10% (corrected for completely hydrolyzed ester, which is unable to couple), while the recovery of the MAb always exceeded 95% (measured by ^{125}I activity).

By adapting the ester concentration during conjugation, conjugates with a ratio >4 could be obtained. However, under these conditions the recovery of the MAb from the PD-10 column dropped significantly, indicating an impairment of the solubility of the MAb.

SDS-PAGE Analysis of ^{131}I-*m*THPC-^{125}I-MAb Conjugates. SDS-PAGE and subsequent CBB staining and Phosphor Imager analysis (Fig. 3) of the conjugate revealed one major protein band and a minor band probably consisting of high molecular weight complexes. Cutting of the gel and dual label counting of the gel pieces showed >90% of the ^{125}I-MAb and >80% of the ^{131}I-*m*THPC to be localized in the main band, when conjugates with a ratio of up to 4 were analyzed. The remaining radioactivity was predominantly localized in the high molecular weight band. A typical example is shown by Figure 3.

***In Vitro* Stability and Immunoreactivity of ^{131}I-*m*THPC-^{125}I-MAb Conjugates.** After 20 h incubation in serum, the ^{131}I-*m*THPC-^{125}I-MAb conjugates were analyzed by SDS-PAGE. Cutting of the gel and subsequent dual label counting showed that the ^{125}I:^{131}I ratio of the IgG peak after incubation in mouse and human serum did not differ from that of the control incubation in 0.9% NaCl. So ^{131}I-*m*THPC-^{125}I-MAb conjugates were fully stable in both serum sources.

Lindmo assays were performed to determine whether coupling of *m*THPC to cMAb U36 or mMAb 425 influenced the immunoreactivity of the MAb. For conjugates with a *m*THPC:MAb ratio of up to 4 no effect on the immunoreactivity was seen in comparison to the unconjugated MAb. Immunoreactivity was >93% in all cases, irrespective whether assessed by ^{125}I or ^{131}I counting.

Biodistribution of ^{131}I-*m*THPC-^{125}I-cMAb U36 conjugates. Dual label experiments were performed to determine whether coupling of ^{131}I-*m*THPC-$(CH_2COOH)_4$ to ^{125}I-cMAb U36 resulted in improved targeting of the sensitizer to the tumor. To this end the biodistribution of unconjugated ^{125}I-cMAb U36 and ^{131}I-*m*THPC-$(CH_2COOH)_4$ were first determined. For evaluation of ^{125}I-cMAb U36, 5 μCi ^{125}I-cMAb U36 (100 μg) were injected in 5 HNX-OE xenograft bearing nude mice. The mice were sacrificed 48 h after injection and the biodistribution was determined. The mean uptake in tumor tissue was 19.5 %ID/g, while the mean blood level was 13.9 %ID/g. Uptake in all other organs was less than 4 %ID/g (Fig. 4A).

For evaluation of *m*THPC-$(CH_2COOH)_4$, 2.5 μCi (5 μg) of ^{131}I-*m*THPC-$(CH_2COOH)_4$ was injected in 5 HNX-OE xenograft bearing nude mice. Figure 4B shows the biodistribution

after 24 h. The compound was cleared very rapidly from the circulation. The mean blood level was 1.5 %ID/g, while the uptake in the tumor was 0.5 %ID/g. Uptake in all other organs was less than 1.5 %ID/g, except for the liver. Because the levels of ^{131}I were already very low after 24 h, the biodistribution after 48 h was not determined.

The biodistribution of ^{131}I-*m*THPC-^{125}I-cMAb U36 conjugates with a ratio of 0.9 and 1.8 is shown in Figure 4C (^{125}I-data) and D (^{131}I-data). Conjugates (100 μg;10 μCi ^{125}I/ 2.5 μCi ^{131}I) were injected in 2 groups of 5 mice and mice were killed 48 h after injection.

The results depicted in Figure 4 revealed that coupling of *m*THPC-$(CH_2COOH)_4$ to cMAb U36 resulted in selective targeting of the sensitizer to the tumor (compare Fig. 4D and B). However, tumor uptake levels of the sensitizer appeared to be lower than could be expected on the basis of the biodistribution of the unconjugated MAb (compare Fig. 4D and A). The fact that tumor uptake of the transporter of the sensitizer, *i.e.* the conjugated MAb, was also lower than expected, indicated that a proportion of the conjugate became rapidly eliminated from the blood (compare blood levels Fig. 4C and A). This elimination was more pronounced for conjugates with the higher *m*THPC:MAb ratio. For both the free *m*THPC-$(CH_2COOH)_4$ and the conjugate, high *m*THPC levels were found in the liver (Fig. 4B and D).

To establish the overall efficiency of sensitizer targeting by the MAb, the biodistribution of unmodified *m*THPC was assessed in the same model as ^{131}I-*m*THPC-$(CH_2COOH)_4$. Externally labeled ^{123}I-*m*THPC (5.0 μg per mouse; specific activity 11.3 Ci/mmol) and internally labeled [^{14}C]*m*THPC (5.0 μg per mouse; specific activity 74 mCi/mmol) were coinjected in 6 HNX-OE bearing nude mice. As previously found by others in BALB/c mice, the free sensitizer showed a random distribution in the organs, and no selective tumor uptake (Fig. 5A and B). For both *m*THPC compounds the highest accumulation was observed in liver, spleen and lung, and the lowest uptake in muscle. Besides this, small differences were observed in the distribution pattern of the compounds, partly originating from the difficulty to assess the [^{14}C] radioactivity in solid/colored tissue.

Photoimmunotherapy *in vitro*. The efficacy of photoimmunotherapy with *m*THPC-cMAb U36 conjugates was tested in 22A cells using the SRB-assay. After exposure to the

relatively high concentration of 1 μM conjugated *m*THPC, about 25% growth inhibition was observed (Fig. 6A). In the same assay unconjugated *m*THPC showed an IC_{50} value of 0.75 nM. Conjugated and free *m*THPC appeared to be non-toxic without illumination.

To investigate the possibility that the sensitizer must be internalized for phototoxicity to occur, we coupled *m*THPC to mMAb 425, an internalizing MAb directed against EGFR. Internalization of the *m*THPC-MAb 425 conjugate was confirmed according by known methods. The efficacy of these conjugates was tested in A431 cells. The IC_{50} value using *m*THPC-mMAb 425 conjugates was 7.3 nM, while in this cell line the IC_{50} value for free *m*THPC was 2.0 nM (Fig. 6B). Once again, conjugated and free *m*THPC were non-toxic without illumination.

Unconjugated cMAb U36 or mMAb 425 did not result in growth inhibition with or without illumination (data not shown).

Favourable results corresponding to the above may be expected from conjugates of m-THPP, m-THPB and m-THPiB and the other porphyrins, chlorins, bacteriochlorins and isobacteriochlorins discussed herein.

COMPOSITIONS AND METHODS OF USE

PDT-immunoconjugates can be parenterally administered in pharmaceutical compositions. Such compositions, comprising of PDT-immunoconjugate e.g.(m-THPC-MAb or m-THPBC-MAb) and a parenterally administrable medium are formulated by methods commonly used in pharmaceutical chemistry. The effective concentration of immunoconjugates of the present invention is dictated by the PDT agent used in the conjugate. One skilled in the art of preparing such compositions will be able to consider optimal ratio of composition of pharmaceutical components and PDT immunoconjugate.

However as one particular example of an injectable solution 20% EtOH, 30% ethylene glycol 400, and 50% water (v/v) with NaCl to give an 0.9% solution (w/v) is made up with

m-THPC-MAb to give a dose of 15 mg for an adult (70kg bodyweight) related to the m-THPC.

Broadly, suitable dose ranges of the m-THPC and the other PDT actives discussed herein are for example 0.1 to 5 mg/kg related to the active.

FURTHER DISCUSSION

Several attempts to use MAbs for selective delivery of photosensitizers to tumors have been made. However, none of these has led to conjugates suitable for therapeutic use. In 1983 the group of Levy described the synthesis of hematoporphyrin-MAb conjugates, but the *in vivo* efficacy of these conjugates appeared to be minimal (14). The same research group developed benzoporphyrin derivative monoacid ring A (BPD)-MAb conjugates, using polyvinyl alcohol as a linker (15), but no data on the therapeutic applicability of these conjugates have been reported. The photosensitizer chlorin e_6 was conjugated to MAbs by the group of Hasan using polyglutamic acid as a linker. Preliminary results of PDT after intraperitoneal injection of these conjugates in a murine intraperitoneal ovarian cancer model showed an improved survival (16). No data on the intravenous use of these conjugates, or for chlorin e_6-MAb conjugates using a dextran polymer linker (17), have been published so far.

Although *m*THPC is one of the most promising photosensitizers available for clinical use, no reports on *m*THPC-MAb conjugates have been published. In this paper a reproducible procedure for conjugation of *m*THPC to MAbs is provided in detail. It is preferred that all reactions, including the modification of *m*THPC, conjugation and subsequent purification, are performed in the dark and that solvents used are saturated with nitrogen. Figure 7 illustrates the phototoxic effect of free *m*THPC, when these precautions are not taken. In this case the integrity of the MAb was impaired in such a way, that it could not penetrate a 7.5% SDS-PAGE gel.

The final route to the reproducible production of *m*THPC-$(CH_2COOH)_3CH_2CO$-TFP was the synthesis of the tetra-esterified compound, followed by partial hydrolysis to leave the mono-ester. The esterification of *m*THPC-$(CH_2COOH)_4$ using an excess of TFP and EDC gave

after column chromatography pure *m*THPC-(CH_2CO-TFP)$_4$ in a reasonable yield (60%). During the following partial hydrolysis procedure, the formation of fully hydrolyzed *m*THPC-(CH_2COOH)$_4$ is unavoidable. When hydrolysis was performed until no di-ester was left, only 20% of the mixture consisted of mono-ester. In our experiments we hydrolyzed till 45% of the mixture consisted of mono-ester. Under these conditions less than 5% di-ester was left, which was judged acceptable for conjugation. As a result, the overall amount of *m*THPC available for conjugation was about 30%, owing to the loss during the modification, esterification and subsequent hydrolysis.

*m*THPC-MAb conjugates prepared according to the method described herein showed a minimal impairment of the integrity on SDS-PAGE (<10% aggregate formation), full stability in serum *in vitro* and an optimal immunoreactivity, provided that not more than 4 *m*THPC molecules were coupled to the MAb. Nevertheless, the pharmacokinetics of *m*THPC-MAb conjugates in xenograft bearing nude mice differed from that of unconjugated MAb. For conjugates with a mean ratio of 0.9 and 1.8, the ^{125}I-levels of the ^{131}I-*m*THPC-^{125}I-MAb in the blood at 48 h p.i. were 69% and 52%, respectively, of that of an unconjugated ^{125}I-MAb. In addition, the ^{131}I-levels decreased more extensively than the ^{125}I-levels. These data indicate that conjugates with a higher ratio are more susceptible for removal from the blood. Our biodistribution data therefore indicate hepatic extraction with retention of the sensitizer in this organ after catabolism. Rapid blood clearance and extensive liver accumulation has also been observed for MAbs coupled with other chemical groups to their lysine residues.

The ^{131}I-*m*THPC-(CH_2COOH)$_4$ was cleared more rapidly from the circulation than the unmodified *m*THPC. The tumor selectivity of MAb-conjugated *m*THPC was increased in comparison with both of these, despite the more rapid elimination of the conjugates with a higher ratio. For the conjugates with a ratio of 0.9 and 1.8 the tumor levels of ^{131}I-*m*THPC were 5.7 and 4.4 %I.D./g, respectively. In absolute amounts this corresponds with 23 and 36 ng/g tumor, respectively. Given the fact that increasing the MAb dose to 400 μg per mouse does not result in antigen saturation, this implies that about 150 ng *m*THPC per g tumor can be delivered.

Another aspect of evaluation is the uptake in the skin, in view of the problem of skin photosensitization. At 48 h after injection the levels of the MAb-conjugated *m*THPC in the skin were much lower than in the tumor (tumor:skin ratio's were 3.5; Fig. 4D). For the unconjugated ^{123}I-*m*THPC and the reference compound [^{14}C]*m*THPC the levels in the skin and tumor were almost the same, 24 h after injection (tumor:skin ratio's were 0.8 and 0.9, respectively; Fig. 5). This is in agreement with data of Whelpton *et al.*, who showed that tumor:skin ratio's remained about 1 between 1 and 4 days after administration of [^{14}C]*m*THPC to Colo 26 bearing mice. Westermann *et al.* showed that in colon carcinoma bearing nude mice these ratio's were improved by using ^{125}I-*m*THPC-PEG conjugates instead of ^{125}I-*m*THPC. The improved selectivity of *m*THPC directed by the MAb does not guarantee improved efficacy. Therefore, *in vitro* studies were performed to compare the phototoxicity of internalizing and non-internalizing MAb-conjugated *m*THPC with that of free *m*THPC at equimolar doses. Our data on the photodynamic efficacy of the *m*THPC-MAb conjugates revealed a remarkable difference between internalizing and non-internalizing MAbs. When coupled to mMAb 425, which was internalized by the cell after conjugation, *m*THPC exhibited more phototoxicity than when coupled to the non-internalizing cMAb U36. Sobolev *et al.* also reported that the photosensitizer chlorin e_6 was more effective when localized intracellularly (18). For BPD-MAb conjugates, produced by the group of Levy, internalization enhanced the cell killing by 10-fold (19). These data strongly suggest that the critical target for photodynamic damage is localized intracellularly. When this is true, it is clear that the kinetics of cellular uptake of free *m*THPC *versus* mMAb 425-conjugated *m*THPC are crucial parameters, and might have influenced the relative efficacy as observed in our SRB experiments (Fig. 6).

ABBREVIATIONS

The abbreviations used are: PDT, photodynamic therapy; *m*THPC, meta-tetrahydroxyphenylchlorin; mMAb/cMAb, murine/chimeric monoclonal antibody; CEA, carcinoembryonic antigen; HNSCC, head and neck squamous cell carcinoma; RIS, radioimmunotherapy; EGFR, epidermal growth factor receptor; ^{1}H-NMR: proton nuclear magnetic resonance; PBS phosphate-buffered saline; HPLC, high-performance liquid chromatography; SDS-PAGE, sodium dodecyl sulfate-polyacrylamide gel electrophoresis; TFP, 2,3,5,6-tetrafluorophenol; EDC, 1-ethyl-3-(3-dimethylaminopropyl)-carbodiimide; BSA,

bovine serum albumin; %ID/g, percentage of injected dose/g of tissue; FCS, fetal calf serum; SRB, sulforhodamine B; HNX-OE, head and neck xenograft line OE.

It may be noted that *m*THPC-(CH_2COOH)$_3CH_2CONH$-MAb conjugates are designated as *m*THPC-MAb conjugates if the modification of *m*THPC is not relevant for understanding

LEGENDS OF FIGURES

Figure 1. Schematic representation of the synthesis of ^{131}I-*m*THPC-(CH_2COOH)$_4$, its esterification, partial hydrolysis and conjugation to a ^{125}I-labeled MAb. It is of note that ^{131}I can occupy 12 positions (both ortho-positions and the para-position relative to the OH, in each of the 4 phenyl rings). In the mono-TFP ester **4**, 1 of the 4 possible mono-TFP esters is depicted.

Figure 2. HPLC profiles (absorbance (415 nm) and radioactivity) during the partial hydrolysis of ^{131}I-*m*THPC-(CH_2CO-TFP)$_4$. At the start, HPLC analysis showed **A** (peak 1: *m*THPC-(CH_2CO-TFP)$_4$) and **B** (peak 1: ^{131}I-*m*THPC-(CH_2CO-TFP)$_4$, peak 1': ^{131}I-*m*THPC-(CH_2CO-TFP)$_3$). During hydrolysis, **C** (peak 1: *m*THPC-(CH_2CO-TFP)$_4$, peak 2: *m*THPC-(CH_2COOH)(CH_2CO-TFP)$_3$, peak 3/4: 2 isomers of *m*THPC-(CH_2COOH)$_2$(CH_2CO-TFP)$_2$, peak 5: *m*THPC-(CH_2COOH)$_3CH_2CO$-TFP and peak 6: *m*THPC-(CH_2COOH)$_4$) and **D** (identical to **C**, corresponding ^{131}I-labeled compounds). Conjugations were performed with mixtures **E** (peak 3/4: 2 isomers of *m*THPC-(CH_2COOH)$_2$(CH_2CO-TFP)$_2$, peak 5: *m*THPC-(CH_2COOH)$_3CH_2CO$-TFP and peak 6: *m*THPC-(CH_2COOH)$_4$) and **F** (identical to **E**, corresponding ^{131}I-labeled compounds).

Figure 3. Example of an SDS-PAGE and Phosphor Imager analysis of a ^{131}I-*m*THPC-^{125}I-cMAb U36 conjugate with ratio 1.8. Quantitative assessment of the radioactivity was obtained by cutting the lane and dual label counting.

Figure 4. Biodistribution of ^{125}I-cMAb U36 and ^{131}I-*m*THPC-(CH_2COOH)$_4$ before and after conjugation. Each preparation was intravenously injected in 6 HNX-OE bearing nude mice. **A**: 48 h p.i. of ^{125}I-cMAb U36 (100 μg; 5 μCi). **B**: 24 h p.i. of ^{131}I-*m*THPC-(CH_2COOH)$_4$ (5 μg; 10 μCi). **C** (^{125}I) and **D** (^{131}I): 48 h p.i. of ^{131}I-*m*THPC-(CH_2COOH)$_3CH_2CONH$-^{125}I-cMAb U36

(100 μg; 5 μCi ^{125}I, 1 μCi ^{131}I) at a molar ratio of 0.9 (open bars) or 1.8 (hatched bars). At indicated time points mice were bled, sacrificed, dissected and the radioactivity levels (%ID/g + SE) of blood, tumor and several organs were assessed. Tu: tumor, Bl: blood, He: heart, Ki: kidney, Sto: stomach, Il: ileum, Co: colon, Ste: sternum, Lu: lung, Mu: muscle, Sk: skin, To: tongue, Li: liver, Sp: spleen.

Figure 5. Comparison of the biodistribution of [^{14}C]*m*THPC (**A**) and ^{123}I-*m*THPC (**B**), 24 h after intravenous injection. Six mice received [^{14}C]-*m*THPC (5.0 μg; 0.54 μCi) and ^{123}I-*m*THPC (5.0 μg; 83 μCi). At 24 h p.i. mice were bled, sacrificed, dissected and the radioactivity levels (%ID/g + SE) of blood, tumor and several organs were assessed. For abbreviations see legend Figure 4.

Figure 6. The SRB assay was used to assess the antiproliferative effect of *m*THPC and *m*THPC-MAb conjugates upon illumination. A) 22A cells, *m*THPC + 25 J/cm^2 (□), *m*THPC not illuminated (•), *m*THPC-cMAb U36 + 25 J/cm^2 (○), *m*THPC-cMAb U36 not illuminated (▲). **B)** A431 cells, *m*THPC + 25 J/cm^2 (□), *m*THPC not illuminated (•), *m*THPC-mMAb 425 + 25 J/cm^2 (○), *m*THPC-mMAb 425 not illuminated (▲). Results of 3 experiments are indicated (means ± SD).

Figure 7. Illustration of the phototoxicity of *m*THPC to the integrity of ^{125}I-cMAb U36. 50 μg ^{125}I-cMAb U36 was incubated in 500 μl MeCN/0.9% NaCl (1/4 v/v) at pH 9.5: with 25 μg *m*THPC in dark (lane A), with 25 μg *m*THPC in light under a N_2 atmosphere (lane B), with 25 μg *m*THPC in light (lane C), without *m*THPC in light as a control (lane D). After 1 h incubation SDS-PAGE and Phosphor Imager analysis was performed.

REFERENCES

1. Dilkes, M. G., DeJode, M. L., Rowntree-Taylor, A., McGilligan, J. A., Kenyon, G. S., and McKelvie, P. *m*THPC photodynamic therapy for head and neck cancer. Lasers Med. Sci., *11:* 23-29, 1996.

2. Savary, J-F., Monnier, P., Fontolliet, C., Wagnières, G., Braichotte, D., and Van den Bergh, H. Photodynamic therapy for early squamous cell carcinomas of the esophagus, bronchi, and mouth with *meta*-tetrahydroxyphenylchlorin. Arch. Otolaryngol. Head Neck Surg., *123:* 162-168, 1997.

3. Quak, J. J., Van Dongen, G. A. M. S., Balm, A. J. M., Brakkee, J. P. G., Scheper, R. J., Snow, G. B., and Meijer, C. J. L. M. A 22-kDa surface antigen detected by monoclonal antibody E48 is exclusively expressed in stratified squamous and transitional epithelia. Am. J. Pathol., *136:* 191-197, 1990.

4. Schrijvers, A. H. G. J., Quak, J. J., Uyterlinde, A. M., Van Walsum, M., Meijer, C. J. L. M., Snow, G. B., and Van Dongen, G. A. M. S. MAb U36, a novel monoclonal antibody successful in immuno-targeting of squamous cell carcinoma of the head and neck. Cancer Res., *53:* 4383-4390, 1993.

5.. De Bree, R., Roos, J. C., Quak, J. J., Den Hollander, W., Van den Brekel, M. W. M., Van de Wal, J. E., Snow, G. B., and Van Dongen, G. A. M. S. Clinical imaging of head and neck cancer with ^{99m}Tc-labeled monoclonal antibody E48 IgG or F(ab')$_2$. J. Nucl. Med., *35:* 775-783, 1994.

6. De Bree, R., Roos, J. C., Quak, J. J., Den Hollander, W., Wilhelm, A. J., Van Lingen, A., Snow, G. B., and Van Dongen, G. A. M. S. Biodistribution of radiolabeled monoclonal antibody E48 IgG and F(ab')$_2$ in patients with head and neck cancer. Clin. Cancer Res., *1:* 277-286, 1995.

7. De Bree, R., Roos, J. C., Quak, J. J., Den Hollander, W., Snow, G. B., and Van Dongen, G. A. M. S. Radioimmunoscintigraphy with ^{99m}Tc-labeled monoclonal antibody U36 and its biodistribution in patients with head and neck cancer. Clin. Cancer Res., *1:* 591-598, 1995.

8. Brakenhoff R. H., Van Gog, F. B., Looney J. E., Van Walsum, M., Snow G. B., and Van Dongen G. A. M. S. Construction and characterization of the chimeric monoclonal antibody E48 for therapy of head and neck cancer. Cancer Immunol. Immunother., *40:* 191-200, 1995.

9. Van Hal N. L. W., Van Dongen, G. A. M. S., Rood-Knippels, E. M. C., Van der Valk, P., Snow, G. B., and Brakenhoff, R. H. Monoclonal antibody U36, a suitable candidate for clinical immunotherapy of squamous-cell carcinoma, recognizes a CD44 isoform. Int. J. Cancer, *68:* 520-527, 1996.

10. Murthy, U., Basu, A., Rodeck, U., Herlyn, M., Ross, A. H., and Das, M. Binding of an antagonistic monoclonal antibody to an intact and fragmented EGR-receptor polypeptide Arch Biochem Biophys., 252: 549-560, 1987.

11. Sunada, H., Magun, B. E., Mendelsohn, J., and MacLeod, C. L. Monoclonal antibody against epidermal growth factor receptor is internalized without stimulating receptor phosphorylation. Proc. Natl. Acad. Sci. USA, *83:* 3825-3829, 1986.

12. Modjtahedi, H., Hickish, T., Nicolson, M., Moore, J., Styles, J., Eccles, S., Jackson, E., Salter, J., Sloane, J., Spencer, L., Priest, K., Smith, I., Dean, C., and Gore, M. Phase I trial and tumor localization of the anti-EGFR monoclonal antibody ICR62 in head and neck or lung cancer. Br. J. Cancer, *73:* 228-235, 1996.

13. Bier, H., Reiffen, K. A., Haas, I., and Stasiecki, P. Dose-dependent access of murine anti-epidermal growth factor receptor monoclonal antibody to tumor cells in patients with advanced laryngeal and hypopharyngeal carcinoma. Eur. Arch. Otorhin., *252:*

14. Mew, D., Wat, C.-K., Towers, G. H. N., and Levy, J. G. Photoimmunotherapy: treatment of animal tumors with tumor-specific monoclonal antibody-hematoporphyrin conjugates. J. Immunol., *130:* 1473-1477, 1983.

15. Davis, N., Liu, D., Jain, A. K., Jiang, S.-Y., Jiang, F., Richter, A., and Levy, J. G. Modified polyvinyl alcohol-benzoporphyrin derivative conjugates as phototoxic agents. Photochem. Photobiol., *57:* 641-647, 1993.

16. Goff, B. A., Blake, J., Bamberg, M. P., and Hasan, T. Treatment of ovarian cancer with photodynamic therapy and immunoconjugates in a murine ovarian cancer model. Br. J. Cancer, *74:* 1194-1198, 1996.

17. Oseroff, A. R., Ohuoha, D., Hasan, T., Bommer, J. C., and Yarmush, M. L. Antibody-targeted photolysis: Selective photodestruction of human T-cell leukemia cells using monoclonal antibody-chlorin e_6 conjugates. Proc. Natl. Acad. Sci. USA, *83:* 8744-8748, 1986.

18. Sobolev A. S., Akhlynina, T. V., Yachmenev, S. V., Rosenkranz, A. A., and Severin, E. S. Internalizable insulin-BSA-chlorin e_6 conjugate is a more effective photosensitizer than chlorin e_6 alone. Biochem. Int., *26:* 445-450, 1992.

19. Jiang, F. N., Allison, B., Liu, D., and Levy J. G. Enhanced photodynamic killing of target cells by either monoclonal antibody or low density lipoprotein mediated delivery systems. J. Controlled Release, *19:* 41-58, 1992.